Energy Conversion

DOI: 10.1002/ange.201301289

# Exceptional Dendrimer-Based Mimics of Diiron Hydrogenase for the Photochemical Production of Hydrogen **

*Tianjun Yu, Yi Zeng,* Jinping Chen, Ying-Ying Li, Guoqiang Yang,* and Yi Li**

The requirement to develop clean and sustainable sources of energy has stimulated new approaches for the conversion and storage of solar energy other than by photovoltaic cells. Of these approaches, the photocatalytic evolution of hydrogen from water is at the forefront.[1] The photochemical production of hydrogen by mimicking natural photosynthesis is considered to be one of the most attractive and potentially useful approaches.[2] In nature, the interconversion of protons and hydrogen is efficiently catalyzed by metalloenzymes known as hydrogenases, which exist in many microorganisms and rely on metals abundant on earth.[3] Since the biological structures and the functionalities of the active sites of hydrogenases were proposed, chemists have made tremendous efforts to model hydrogenases for energy conversion.[4] Of these modeling studies, those on diiron hydrogenase have inspired further research, and analogues of the active sites of hydrogenase have been developed that have high fidelity and result in a significant improvement in the catalytic interconversion of $H_2$ and $H^+$.[5] Diiron hydrogenase mimics for the photochemical production of hydrogen have been constructed by various strategies.[6] However, only a few systems have reached turnovers on the order of hundreds and turnover frequencies of several hundreds per hour under visible light irradiation.[7] Recently, a hybrid system comprising ZnS and a hydrogenase mimic driven by UV light resulted in turnovers of over 2600 being obtained.[8] The reported quantum yields for the diiron hydrogenase mimic are just a few percent. Therefore, the construction of robust hydrogenase models with high photocatalytic activity and efficiency remains a great challenge.

As is the case with most natural enzymes, the active site of hydrogenase is buried within a protein matrix that modulates the reactivity and protects the active center so as to facilitate catalysis (Figure 1 a).[3] Inspired by the natural enzymes, a hydrogenase mimic may be constructed by utilizing the distinct architecture of a dendrimer. Dendrimers are well-defined and hierarchically branched macromolecules which

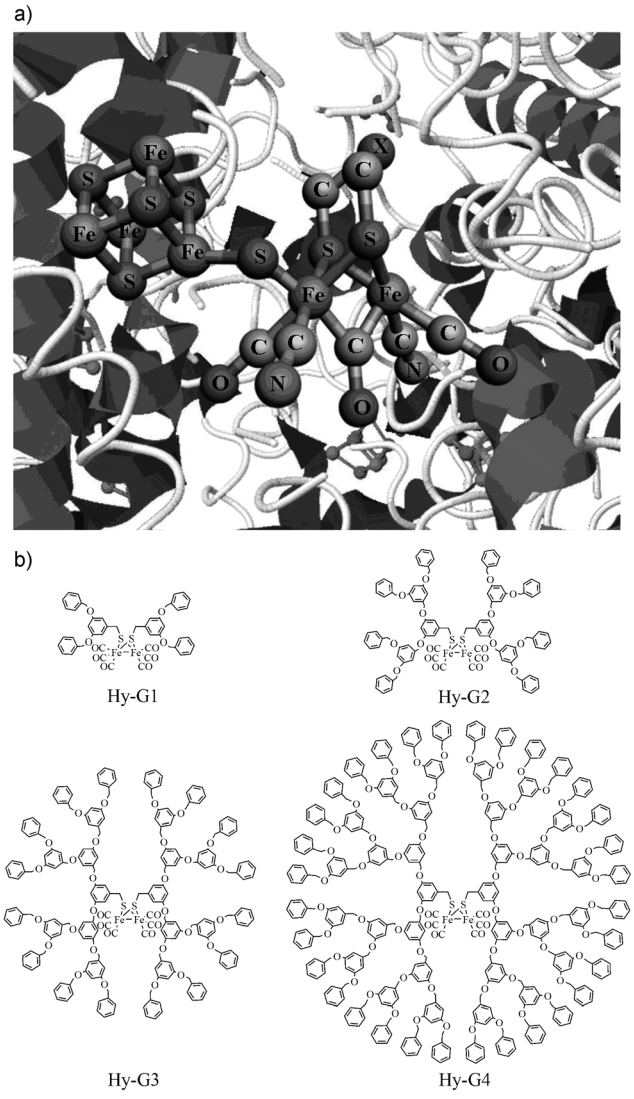


***Figure 1.*** a) Schematic illustration of the active site of diiron hydrogenase encapsulated in a protein matrix, derived from protein crystallographic database. X = $CH_2$, NH, O. b) Structures of dendritic hydrogenase mimics Hy-G*n* (*n* = 1–4) bearing $\{(\mu\text{-S})_2Fe_2(CO)_6\}$, a model of the active site of hydrogenase, as the catalytic center (asymmetry of the sulfur–carbon bond is omitted).

[*] Dr. T. J. Yu, Dr. Y. Zeng, Dr. J. P. Chen, Dr. Y. Y. Li, Prof. Dr. Y. Li
Key Laboratory of Photochemical Conversion and Optoelectronic Materials
Technical Institute of Physics and Chemistry
Chinese Academy of Sciences
Beijing 100190 (P. R. China)
E-mail: yili@mail.ipc.ac.cn
zengyi@mail.ipc.ac.cn
Prof. Dr. G. Q. Yang
Beijing National Laboratory for Molecular Sciences
Key Laboratory of Photochemistry, Institute of Chemistry
Chinese Academy of Sciences
Beijing 100190 (P. R. China)
E-mail: gqyang@iccas.ac.cn

[**] We are grateful for funding from the 973 program (nos. 2013CB834505, 2013CB834700, 2010CB934500), the National Natural Science Foundation of China (grant nos. 21173245, 21073215, 21004072, 21002109, 21233011, and 21273258), and the Solar Energy Initiative of the Chinese Academy of Sciences.

Supporting information for this article is available on the WWW under http://dx.doi.org/10.1002/anie.201301289.



© 2013 Wiley-VCH Verlag GmbH & Co. KGaA, Weinheim

have widespread applications in enzyme mimics, catalysts, and biomedical materials.[9] Much effort from our research group in recent years has been devoted to dendritic mimics of the natural light harvesting complex for photochemical conversion.[10] Here we report bio-inspired hydrogenase mimics with dendritic architectures that encapsulate the active-site model of diiron hydrogenase at the core and demonstrate unprecedented catalytic photochemical production of hydrogen in a homogeneous system.

The hydrogenase mimics (Hy-G*n*; generation number $n = 1$–4) were constructed by attaching two Fréchet-type dendrons (G*n*, $n = 1$–4)[11] to a $\{(\mu\text{-}S_2)Fe_2(CO)_6\}$ subunit (Figure 1b), one of the most common and primitive [2Fe2S] clusters used in mimics of the active site of diiron hydrogenase. $[(\mu\text{-}S_2)Fe_2(CO)_6]$ was treated with $LiBHEt_3$ in tetrahydrofuran and subsequently treated with different generations of dendron bromides to give the corresponding artificial hydrogenase. The structures of the synthetic hydrogenase mimics were characterized by NMR and IR spectroscopy as well as mass spectrometry (see the Supporting Information). The IR spectra of Hy-G*n* are similar, and the three bands of $\nu$(CO) at 1989, 2033, and 2069 $cm^{-1}$ show negligible shifts in the different generations, thus indicating the relative independence of the electronic state of the [2Fe2S] core on the dendrimer generation (see Figure S3 in the Supporting Information). The identical absorption spectra of Hy-G*n* in the visible region, where the absorption of the [2Fe2S] unit lies, also suggest that there is no measurable interaction between the dendrons and the [2Fe2S] core of Hy-G*n* in the ground state (see Figure S5 in the Supporting Information).

The photocatalytic evolution of hydrogen by the synthetic hydrogenase mimics was examined by adopting a three-component homogeneous catalyst system. This system comprises $[Ir(ppy)_2(bpy)]PF_6$ (ppy = 2-phenylpyridine, bpy = 2,2′-bipyridine) as the photosensitizer to absorb light, Hy-G*n* as the proton reduction catalyst, and triethylamine (TEA) as the sacrificial electron donor (Figure 2). A solvent mixture of acetone and water was used to solubilize all the components. Irradiation of the catalyst system with visible light resulted in the immediate production of hydrogen, which was quantified by gas chromatography, with the turnover numbers (TONs) calculated from the amount of $H_2$ molecules generated versus the number of artificial hydrogenase molecules. Control experiments in the absence of Hy-G*n* showed no detectable photochemical production of $H_2$, thus verifying that the dendritic diiron complex is essential for the photocatalytic evolution of $H_2$. The performance of the photocatalyst system was dramatically affected by the reaction conditions, such as the water content of the solvent mixture as well as the concentrations of Hy-G*n* and TEA. An optimization of the reaction conditions was conducted to improve the efficiency of the photochemical production of $H_2$ (see Table S1 in the Supporting Information).

An acetone/water ratio of 9:1 results in the best catalytic activity when all the other conditions are kept identical. The optimal concentrations of the catalyst and TEA were confirmed to be approximately 1 μM and 0.6 M, respectively, with $Ir^{III}$ complex at 0.5 mM. The photocatalytic performance of Hy-G*n* ($n = 1$–4) was evaluated upon irradiation with visible light from a xenon lamp (16 mW $cm^{-2}$) under the optimal conditions; the TONs over the course of the irradiation are depicted in Figure 3. $H_2$ was generated rapidly

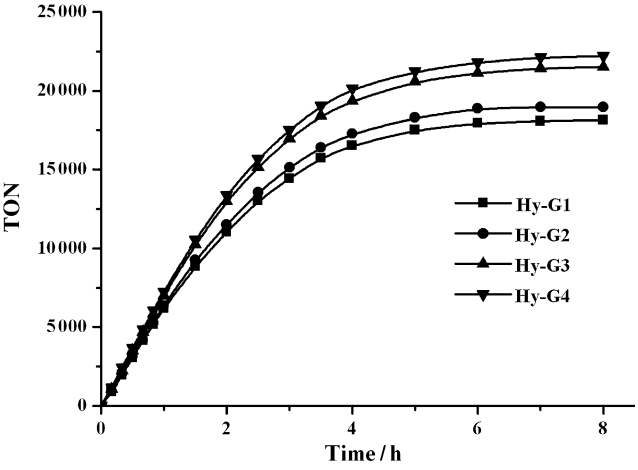


***Figure 3.*** Photochemical production of hydrogen by the Hy-G*n* catalysts. Turnover numbers versus time during $H_2$ production by the Hy-G*n* catalysts in an acetone/water mixture (9:1, v/v) under irradiation with visible light (16 mW $cm^{-2}$). The concentrations of Hy-G*n*, the $Ir^{III}$ complex, and TEA are 1 μM, 0.5 mM, and 0.6 M, respectively.

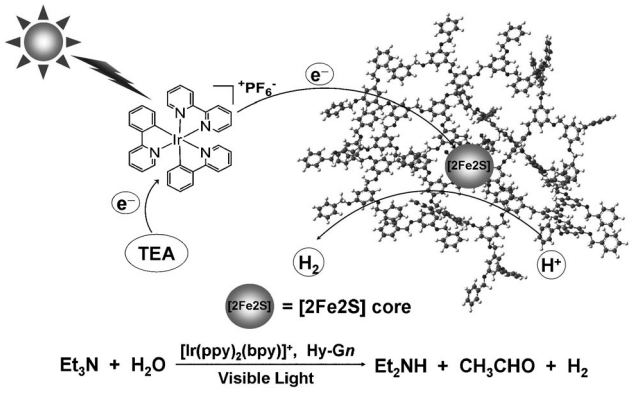


***Figure 2.*** The homogeneous photocatalytic system. Hy-G4 acts as the catalyst for the photochemical generation of $H_2$.

in all four photocatalytic systems during the first 1 h of irradiation, with initial turnover frequencies (TOFs) of up to 6190, 6360, 7000, and 7240 $h^{-1}$ for the dendritic diiron complex of generations 1–4, respectively. The evolution of $H_2$ slowed down gradually with prolonged irradiation time, and reached a maximum plateau after about 8 h irradiation. The corresponding TONs were up to 18100, 19000, 21500, and 22200 for the hydrogenase mimics of generations 1–4, respectively. The increase in the initial TOF and TON with an increase in the catalyst generation indicates that the catalytic activity and stability of the catalyst were improved by the dendritic frameworks. These TOF and TON values represent the highest efficiency and stability to date for $H_2$ evolution based on [2Fe2S] catalysts. The cessation of the $H_2$ production is mainly attributed to the inactivation of the catalysts, as


© 2013 Wiley-VCH Verlag GmbH & Co. KGaA, Weinheim

evident from the recovery of the catalysis on adding more dendritic complexes. Moreover, the decomposition of the $Ir^{III}$ complex also accounts for the decrease in the $H_2$ production rates, because re-addition of the photosensitizer is needed to fully recover the efficiency of the catalyst systems.

The catalysts are most active at low concentrations. Figure 4 shows the effect of concentration on the rate and overall evolution of hydrogen in the case of Hy-G3, with an increase observed as the catalyst concentration increases. The initial rate of hydrogen evolution, which is calculated from the first hour of illumination, is proportional to the catalyst concentration when the catalyst concentration is $\leq 0.5$ μM, but does not increase linearly with the catalyst concentration at $> 0.5$ μM (inset of Figure 4). This finding can be rationalized by the limitation in the amount of reductive photosensitizer (the reductive quenching mechanism is discussed below), and further confirmed by the dependence of the hydrogen evolution on the intensity of the irradiation. When we decreased the illumination intensity from 16 mW cm$^{-2}$ to 4 mW cm$^{-2}$, the initial rate for hydrogen evolution decreased markedly (see Figure S6 in the Supporting Information). When the intensity of the irradiation is reduced, fewer photons are absorbed by the catalyst system, which reduces the amount of reductive photosensitizer formed; consequently, the initial rate of hydrogen evolution decreases. However, more intense illumination also does not benefit the catalytic performance (see Figure S6 in the Supporting Information). Under the intense illumination, the catalyst system demonstrates a higher TOF at the cost of shortening the working time, which may be attributed to photochemical damage of the catalyst and the photosensitizer. When the irradiation is too weak, the catalytic rate is lowered and a gradual decomposition of the catalyst and the sensitizer may be the cause of the lower performance of the catalyst.

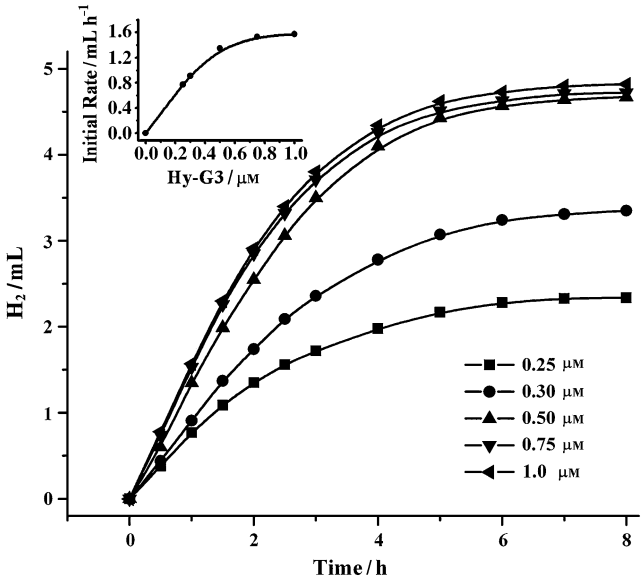


***Figure 4.*** Photocatalytic evolution of $H_2$ in acetone/$H_2O$ = 9:1 with different concentrations of Hy-G3. Hydrogen production was calculated on the basis of the amount of hydrogen generated in 10 mL of the sample solution over 8 h irradiation (16 mW cm$^{-2}$). [Ir(ppy)$_2$(bpy)$PF_6$] = $5 \times 10^{-4}$ M, [TEA] = 0.6 M, [Hy-G3] = 0.25–1.0 μM. Inset: Initial rate of hydrogen evolution versus [Hy-G3].

The quantum yields of hydrogen evolution were measured by irradiation of the solutions under the optimal conditions (Hy-G$n$ = 1 μM, $Ir^{III}$ complex = 0.5 mM, TEA = 0.6 M in 10 mL acetone/$H_2O$ = 9:1) with a laser operating at a wavelength of 440 nm for 2 h. The quantum yields were determined to be 0.18, 0.21, 0.24, and 0.28 for Hy-G$n$ of generations 1–4, respectively, which means that of the 100 photons absorbed by the photosensitizer, 18–28 photons are stored as chemical energy. These are the best quantum yields for [2Fe2S]-based catalysts so far.

The photocatalytic evolution of $H_2$ from the homogeneous three-component systems involves a photosensitizing mechanism which begins with excitation of the photosensitizer followed by delivery of an electron to the catalyst, either by direct oxidative quenching or after reduction by the sacrificial electron donor.[12] An estimation of the change in the free energy $\Delta G$ indicated that direct electron transfer from the excited photosensitizer $*[Ir(ppy)_2(bpy)]^+$ to the [2Fe2S] core of Hy-G$n$ ($n$ = 1–4) is thermodynamically unfavorable (see Table S3 in the Supporting Information). Alternatively, $*[Ir(ppy)_2(bpy)]^+$ can be reductively quenched by TEA to generate a reduced photosensitizer $[Ir(ppy)_2(bpy)]$, which is sufficiently reductive (based on the $\Delta G$ value derived from the reduction potentials) to donate an electron to the [2Fe2S] center (i.e. $Fe^IFe^I$), thereby generating $[2Fe2S]^-$ (i.e. $Fe^0Fe^I$). Therefore, we infer that the electron transfer occurs between the reduced photosensitizer and the [2Fe2S] center, which is further validated by transient absorption spectroscopy studies. Pulsed laser photolysis of the photosensitizer in the presence of TEA shows an intense transient absorption of $*[Ir(ppy)_2(bpy)]^+$ with a maximum at 380 nm. The decay of this species is accompanied by a rise of new absorption bands at around 390 and 530 nm, which are assigned to the reduced species $[Ir(ppy)_2(bpy)]$ (see Figures S9 and S11 in the Supporting Information). The transient absorption of $[Ir(ppy)_2(bpy)]$ decays faster when the dendritic catalyst is added to the system, and a new shoulder at around 400 nm appears, which is assigned on the basis of spectroelectrochemical observations to the reduced catalyst core $[2Fe2S]^-$ (see Figures S10 and S12 in the Supporting Information). A control experiment in the absence of TEA shows no formation of the reduced species of either the photosensitizer or the catalyst (see Figure S13 in the Supporting Information), thus confirming that the excited photosensitizer is reductively quenched by the sacrificial electron donor first and then oxidized by the catalyst. After quenching the photosensitizer, TEA undergoes decomposition to produce a proton, acetaldehyde, and diethylamine in the presence of water.[13]

Effective charge separation has been considered to be a key factor for both natural photosynthesis and artificial photochemical conversion.[2a,14] The increase in the initial rate and quantum yield of hydrogen evolution as the dendrimer generation of the catalyst increases can be interpreted by the lifetimes of the charge-separated states. These lifetimes were obtained by analyzing the kinetic traces by transient absorp-

 © 2013 Wiley-VCH Verlag GmbH & Co. KGaA, Weinheim 

tion spectroscopy at 400 nm. In the absence of the catalyst, the kinetic trace at 400 nm fits well with a monoexponential process, thus giving the lifetime of the reduced photosensitizer $[Ir(ppy)_2(bpy)]$ as 5.3 ms (see Figure S11 in the Supporting Information). When Hy-G*n* is present, the kinetic trace at 400 nm can only be fitted with a double exponential process because of the evident absorption overlap of $[Ir(ppy)_2(bpy)]$ and $[2Fe2S]^-$, and gives two lifetimes (see Figure S12 in the Supporting Information): the one in milliseconds is assigned to $[Ir(ppy)_2(bpy)]$, which is shorter than 5.3 ms because of electron transfer from $[Ir(ppy)_2(bpy)]$ to the [2Fe2S] core, and the other in microseconds is attributed to the charge-separated state $[2Fe2S]^-$, which was determined to be 27.2, 42.4, 66.1, and 86.3 μs for Hy-G*n* of generations 1–4, respectively (see Table S4 in the Supporting Information). The increase in the lifetime of the charge-separated state can be attributed to the contribution made by the dendritic frameworks. The site isolation effect stabilized the encapsulated $[2Fe2S]^-$ unit that is formed, thereby resulting in an enhanced catalyst performance as the generation number increases.[15]

Generally, electron transfer requires strong electronic orbital overlap between a donor and an acceptor, and therefore the thick dendritic framework of the higher generation catalysts should hinder the electron transfer between the $[Ir(ppy)_2(bpy)]$ and the [2Fe2S] core, and consequently results in a decrease in the hydrogen evolution. However, in the present study, the higher generation catalyst is more catalytically active, which suggests that the dendritic structure plays a positive role in the catalytic process. Compared with the bulk polar solvent, the dendritic structure provides a hydrophobic microenvironment. The neutral reduced photosensitizer $[Ir(ppy)_2(bpy)]$ prefers to penetrate into the dendritic interior, thereby resulting in electron transfer with the [2Fe2S] unit. After the electron transfer, the photosensitizer species is restored to its cationic form $[Ir(ppy)_2(bpy)]^+$ and tends to escape from the dendritic architecture into the polar solvent phase, which suppresses the unwanted back electron transfer and facilitates the evolution of hydrogen.

Moreover, the better catalytic performance of the higher generation catalyst suggests a possible unimolecular catalytic mechanism. The charge-separated state $Fe^0Fe^I$ needs to react with a proton to form an $H{\cdot}Fe^{II}Fe^I$ intermediate so that the catalytic process may continue. However, to obtain $H_2$, the transfer of a second electron to the diiron core and the total uptake of two protons are necessary. The precise mechanism of the further reduction of the diiron core and formation of dihydrogen is still ambiguous for hydrogenase mimics because the intermediates remain spectroscopically uncharacterized. Multiple mechanistic pathways have been proposed for the production of $H_2$ based on the high catalytic activities.[12a,16] The experiments on the relationship between the rate of $H_2$ evolution and the catalyst concentration were conducted in the present study. The rate of $H_2$ evolution increases linearly with an increasing concentration of Hy-G3 in the low concentration region when other reaction conditions are kept identical (inset of Figure 4). This finding indicates that $H_2$ is probably not generated through bimolecular or disproportional catalysis, but possibly through a unimolecular catalytic pathway. $H{\cdot}Fe^{II}Fe^I$ can be reduced and protonated successively, thereby resulting in the production of $H_2$ and recovery of $Fe^IFe^I$, or undergo a secondary protonation to form a dihydride intermediate that undergoes a subsequent reduction and $H_2$ liberation.[6a]

In summary, our observations on dendritic hydrogenase mimics with remarkably high quantum yield, turnover numbers, and turnover frequency demonstrate a promising approach toward the conversion of solar energy into hydrogen. The catalytic center demonstrates high catalytic activities and the dendritic frameworks provide a distinct microenvironment to regulate the electron-transfer process and protect the active site, similar to natural proteins, thus consequently advancing the photocatalysis. The experiment design shown here provides an unsophisticated way to construct promising photocatalysts as well as artificial photosynthesis systems.

Received: February 13, 2013
Published online: April 15, 2013

**Keywords:** dendrimers · energy conversion · hydrogen · hydrogenases · photochemistry

[1] T. R. Cook, D. K. Dogutan, S. Y. Reece, Y. Surendranath, T. S. Teets, D. G. Nocera, *Chem. Rev.* **2010**, *110*, 6474 – 6502.

[2] a) A. Magnuson, M. Anderlund, O. Johansson, P. Lindblad, R. Lomoth, T. Polivka, S. Ott, K. Stensjo, S. Styring, V. Sundstrom, L. Hammarstrom, *Acc. Chem. Res.* **2009**, *42*, 1899 – 1909; b) D. Gust, T. A. Moore, A. L. Moore, *Acc. Chem. Res.* **2009**, *42*, 1890 – 1898; c) W. Lubitz, E. J. Reijerse, J. Messinger, *Energy Environ. Sci.* **2008**, *1*, 15 – 31.

[3] J. C. Fontecilla-Camps, P. Amara, C. Cavazza, Y. Nicolet, A. Volbeda, *Nature* **2009**, *460*, 814 – 822.

[4] a) M. L. Helm, M. P. Stewart, R. M. Bullock, M. R. DuBois, D. L. DuBois, *Science* **2011**, *333*, 863 – 866; b) H. I. Karunadasa, C. J. Chang, J. R. Long, *Nature* **2010**, *464*, 1329 – 1333; c) A. Le Goff, V. Artero, B. Jousselme, P. D. Tran, N. Guillet, R. Metaye, A. Fihri, S. Palacin, M. Fontecave, *Science* **2009**, *326*, 1384 – 1387.

[5] a) J. M. Camara, T. B. Rauchfuss, *Nat. Chem.* **2012**, *4*, 26 – 30; b) O. F. Erdem, L. Schwartz, M. Stein, A. Silakov, S. Kaur-Ghumaan, P. Huang, S. Ott, E. J. Reijerse, W. Lubitz, *Angew. Chem.* **2011**, *123*, 1475 – 1479; *Angew. Chem. Int. Ed.* **2011**, *50*, 1439 – 1443; c) M. L. Singleton, J. H. Reibenspies, M. Y. Darensbourg, *J. Am. Chem. Soc.* **2010**, *132*, 8870 – 8871; d) C. Tard, C. J. Pickett, *Chem. Rev.* **2009**, *109*, 2245 – 2274; e) F. Gloaguen, T. B. Rauchfuss, *Chem. Soc. Rev.* **2009**, *38*, 100 – 108; f) G. A. N. Felton, A. K. Vannucci, J. Z. Chen, L. T. Lockett, N. Okumura, B. J. Petro, U. I. Zakai, D. H. Evans, R. S. Glass, D. L. Lichtenberger, *J. Am. Chem. Soc.* **2007**, *129*, 12521 – 12530; g) C. Tard, X. M. Liu, S. K. Ibrahim, M. Bruschi, L. De Gioia, S. C. Davies, X. Yang, L. S. Wang, G. Sawers, C. J. Pickett, *Nature* **2005**, *433*, 610 – 613; h) M. Y. Darensbourg, E. J. Lyon, X. Zhao, I. P. Georgakaki, *Proc. Natl. Acad. Sci. USA* **2003**, *100*, 3683 – 3688; i) M. Wang, L. Chen, L. C. Sun, *Energy Environ. Sci.* **2012**, *5*, 6763 – 6778.

[6] a) W. Wang, T. B. Rauchfuss, L. Bertini, G. Zampella, *J. Am. Chem. Soc.* **2012**, *134*, 4525 – 4528; b) M. R. Wasielewski, A. P. S. Samuel, D. T. Co, C. L. Stern, *J. Am. Chem. Soc.* **2010**, *132*, 8813 – 8815; c) A. M. Kluwer, R. Kapre, F. Hartl, M. Lutz, A. L. Spek, A. M. Brouwer, P. W. N. M. van Leeuwen, J. N. H. Reek, *Proc. Natl. Acad. Sci. USA* **2009**, *106*, 10460 – 10465; d) Y. Na, M.

 © 2013 Wiley-VCH Verlag GmbH & Co. KGaA, Weinheim 

Wang, J. X. Pan, P. Zhang, B. Akermark, L. C. Sun, *Inorg. Chem.* **2008**, *47*, 2805 – 2810; e) L. C. Song, M. Y. Tang, F. H. Su, Q. M. Hu, *Angew. Chem.* **2006**, *118*, 1148 – 1151; *Angew. Chem. Int. Ed.* **2006**, *45*, 1130 – 1133; f) S. Ott, M. Kritikos, B. Akermark, L. C. Sun, *Angew. Chem.* **2003**, *115*, 3407 – 3410; *Angew. Chem. Int. Ed.* **2003**, *42*, 3285 – 3288; g) Y. Sano, A. Onoda, T. Hayashi, *Chem. Commun.* **2011**, *47*, 8229 – 8231; h) X. Li, M. Wang, D. Zheng, K. Han, J. Dong, L. Sun, *Energy Environ. Sci.* **2012**, *5*, 8220 – 8224; i) Y. Sano, A. Onoda, T. Hayashi, *J. Inorg. Biochem.* **2012**, *108*, 159 – 162; j) A. Roy, C. Madden, G. Ghirlanda, *Chem. Commun.* **2012**, *48*, 9816 – 9818.,

[7] a) F. Wang, W.-G. Wang, X.-J. Wang, H.-Y. Wang, C.-H. Tung, L.-Z. Wu, *Angew. Chem.* **2011**, *123*, 3251 – 3255; *Angew. Chem. Int. Ed.* **2011**, *50*, 3193 – 3197; b) M. Wang, P. Zhang, Y. Na, X. Q. Li, Y. Jiang, L. C. Sun, *Dalton Trans.* **2010**, *39*, 1204 – 1206; c) D. Streich, Y. Astuti, M. Orlandi, L. Schwartz, R. Lomoth, L. Hammarstrom, S. Ott, *Chem. Eur. J.* **2010**, *16*, 60 – 63.

[8] F. Y. Wen, X. L. Wang, L. Huang, G. J. Ma, J. H. Yang, C. Li, *ChemSusChem* **2012**, *5*, 849 – 853.

[9] a) D. Astruc, *Nat. Chem.* **2012**, *4*, 255 – 267; b) L. Röglin, E. H. M. Lempens, E. W. Meijer, *Angew. Chem.* **2011**, *123*, 106 – 117; *Angew. Chem. Int. Ed.* **2011**, *50*, 102 – 112; c) C. Liang, J. M. J. Fréchet, *Prog. Polym. Sci.* **2005**, *30*, 385 – 402; d) D. L. Jiang, T. Aida, *Prog. Polym. Sci.* **2005**, *30*, 403 – 422; e) S. M. Grayson, J. M. J. Fréchet, *Chem. Rev.* **2001**, *101*, 3819 – 3867; f) M. Zhao, B. Helms, E. Slonkina, S. Friedle, D. Lee, J. DuBois, B. Hedman, K. O. Hodgson, J. M. J. Fréchet, S. J. Lippard, *J. Am. Chem. Soc.* **2008**, *130*, 4352 – 4363.

[10] a) T. Yu, W. Wang, J. Chen, Y. Zeng, Y. Li, G. Yang, Y. Li, *J. Phys. Chem. C* **2012**, *116*, 10516 – 10521; b) Y. Zeng, Y. Y. Li, J. P. Chen, G. Q. Yang, Y. Li, *Chem. Asian J.* **2010**, *5*, 992 – 1005; c) Y. Zeng, Y. Y. Li, M. Li, G. Q. Yang, Y. Li, *J. Am. Chem. Soc.* **2009**, *131*, 9100 – 9106; d) J. P. Chen, S. Y. Li, L. Zhang, B. N. Liu, Y. B. Han, G. Q. Yang, Y. Li, *J. Am. Chem. Soc.* **2005**, *127*, 2165 – 2171.

[11] C. J. Hawker, J. M. J. Fréchet, *J. Am. Chem. Soc.* **1990**, *112*, 7638 – 7647.

[12] a) R. Lomoth, S. Ott, *Dalton Trans.* **2009**, 9952 – 9959; b) W. N. Cao, F. Wang, H. Y. Wang, B. Chen, K. Feng, C. H. Tung, L. Z. Wu, *Chem. Commun.* **2012**, *48*, 8081 – 8083; c) S. P. Luo, E. Mejia, A. Friedrich, A. Pazidis, H. Junge, A. E. Surkus, R. Jackstell, S. Denurra, S. Gladiali, S. Lochbrunner, M. Beller, *Angew. Chem.* **2013**, *125*, 437 – 441; *Angew. Chem. Int. Ed.* **2013**, *52*, 419 – 423.

[13] M. J. Esswein, D. G. Nocera, *Chem. Rev.* **2007**, *107*, 4022 – 4047.

[14] P. Poddutoori, D. T. Co, A. P. S. Samuel, C. H. Kim, M. T. Vagnini, M. R. Wasielewski, *Energy Environ. Sci.* **2011**, *4*, 2441 – 2450.

[15] a) M. Hara, S. Samori, X. C. Cai, S. Tojo, T. Arai, A. Momotake, J. Hayakawa, M. Uda, K. Kawai, M. Endo, M. Fujitsuka, T. Majima, *J. Am. Chem. Soc.* **2004**, *126*, 14217 – 14223; b) M. Kawa, J. M. J. Fréchet, *Chem. Mater.* **1998**, *10*, 286 – 296.

[16] F. Wang, W. G. Wang, H. Y. Wang, G. Si, C. H. Tung, L. Z. Wu, *ACS Catal.* **2012**, *2*, 407 – 416.

 © 2013 Wiley-VCH Verlag GmbH & Co. KGaA, Weinheim 